IEEE Access
Multidisciplinary | Rapid Review | Open Access Journal

Received April 1, 2019, accepted April 26, 2019, date of publication May 1, 2019, date of current version May 17, 2019.

Digital Object Identifier 10.1109/ACCESS.2019.2914427

Emergence of Persistent Activity States in a Two-Population Neural Field Model for Smooth α-Type External Input

ZEESHAN AFZAL[1], YONGSHENG RAO[2], YOUSAF BHATTI[1], AND NAIMA AMIN[3]
[1]Department of Mathematics, COMSATS University Islamabad, Lahore Campus, Lahore 54000, Pakistan
[2]Institute of Computing Science and Technology, Guangzhou University, Guangzhou 510006, China
[3]Department of Physics, COMSATS University Islamabad, Lahore Campus, Lahore 54000, Pakistan

Corresponding author: Yongsheng Rao (rysheng@gzhu.edu.cn)

This work was supported in part by the National Key R&D Program of China under Grant 2018YFB1005104, in part by the National Natural Science Foundation of China under Grant 11701118, in part by the Specialized Fund for Science and Technology Platform and Talent Team Project of Guizhou Province under Grant QianKeHePingTaiRenCai [2016]5609, and in part by the Higher Education Commission under Grant NRPU-5346 by HEC.

ABSTRACT We investigate the emergence of localized activity states, so-called bumps in Wilson–Cowan type two-population neural field model under the influence of transient spatio-temporal external input with smooth α-type temporal function. This two-population model is composed of two coupled nonlinear differential equations derived for the dynamics of spatially localized populations of both excitatory and inhibitory model neurons. The model with no external input corresponds to at most two bump pair solutions. Such a system can be interpreted as a minimal cortical model for short term working memory, that is the ability of the brain to actively hold stimulus-related information for some seconds in short term memory and discards once it becomes irrelevant Initially, if there is no activity in the system, persistent activity state can be evoked by switching on a suitable transient excitatory external input. This activity remains stable even though external input is switched off. The effect of external input on the emergence of bumps for different spatial and smooth α-type temporal functions of external input is investigated and found that certain parameters play a key role in the generation of persistent activity states in the network, e.g., relative inhibition time constant, total duration, and the amplitude of external input. It is found that the minimum values of the amplitude and active time to evoke the activity in the network is smaller than those observed in Yousaf *et al.* showing that the present choice of temporal function in the external input is more effective and more close to natural behavior.

INDEX TERMS Two population neuronal networks, stationary symmetric solutions, integro-differential equations, Runge-Kutta Fourth order method.

I. INTRODUCTION

The brain has a basic ability to transiently hold stimulus related information so-called working memory It has been observed experimentally, that persistent evoking of groups of neurons in prefrontal cortex were identified as a neural correlate underlying this short-term memory [5], [11], [12], [22], [23].

In last decade studies have been done where various models have come across on how cortical networks can possibly generate and sustain the selective activation of group of neurons (subpopulations), e.g. attractor states in the network, persistent activation of thalmo-cortical and cortiocortical loops [12], [13]. Especially, the idea of network attractor states in framework of neural field models investigated intensively in many studies (e.g., [3], [4], [6], [14], [16], [18], [20], [25], [27]) Working memory are generally discussed the disjoint classes on how the persistent states of activity is generated. One most popular mechanism, in the cell assembly the activity is persistent through strong recurrent excitatory connections [21]. Another idea is that activity circulates in form loops (called synfire chains) [22], which consists of feed-forward connected subgroups with no direct feedback links between succeeding groups of neurons. These models

The associate editor coordinating the review of this manuscript and approving it for publication was Aniruddha Datta.

can also be distinguished on the basis of discrete attractor states associated discrete memory items and models that support persistent attractor states associated continuous variables like space.

Sufficient excitatory feedback is an important element for stable persistent activation in the network, while the role of inhibition is required in order to keep the system from entering a state of run-away excitation [31]–[33]. This can be achieved by assuming a Mexican hat type connectivity functions in neural field models. Such systems with the assumption of translation invariant coupling property can sustain a stable activation of a localized subpopulation of the network (bump attractor) [1], [8], [14], [16], [27], [29]. A large number of modeling studies have been made to investigate the generation of coherent structures such as stationary bumps, their existence, uniqueness and stability [7], [24]–[26], [28], [36], [38], [40]. However the key property of these models is to explain the emergence of persistent activity in response to external stimulus and neural field models have provided a powerful tool to investigate these properties.

In 1970's Amari [27] investigated the stability and existence of bumps in a simplified rate model of lateral inhibition type subject to uniform external input in one spatial dimension. Latter on Kishimoto and Amari [37] also addressed the same issues with a different firing rate functions. Laing *et al.* [29] extended the work of Amari [27] by using the connectivity function in replace of Mexican hat connectivity function. They also proved the non-existence of multi-bump solutions for Mexican hat shape connectivity function. A stable multi bump solution is generated for the two dimensional case.

Rubin and Troy [32] have shown the existence of bumps and linear stability in one population neuronal models without recurrent excitations. They use alternate approach of recurrent excitation is off-center synaptic architecture subject to the constant external input. They investigated the existence of bumps (Stationary symmetric solution), shapes and the mechanism that forms the bumps.

Olyanic *et al.* generalized this work for more class of temporal kernels [16]. Yousaf *et al.* [3] investigated bump pair formation under the effect of spatially dependent and temporally transient external input in two-population neuronal model. In this new scenario, different properties of model e.g. boundedness, existence, uniqueness and the necessary condition for emergence of the activity were studied. These investigations are performed under the influence of spatio-temporal external input with triangular temporal part.

The triangular type external input is also observed by [34] but the smooth external input is more realistic choice for temporal part as observed in Roth *et al.* [2], where axonal calcium imaging technique is to measure the information provided visual cortex by the pulvinar equivalent in mice, the lateral posterior nucleus (LP), as well as the dorsolateral geniculate nucleus (dLGN). In [2], they have discussed the thalamic inputs. Mathematically, these inputs can be depicted by the Alpha function. The main objective of this study is to investigate the effect of spatio-temporal external input on bump solutions with more smooth and more commonly observed temporal part. In order to have a control of the Alpha function we slightly modify it and name it as α-type function which is given by (26). In order to investigate the effect of each part of the external input on the self-sustained activity states, we split the external input into three parts amplitude, spatial profile and the temporal one. In view of the observations of [2] and the fact that **stationary symmetric solution** serves as a working memory in the network, it will be of great interest to investigate the emergence of these states for the present choice of temporal function in the external input. The paper is organized in the following way:

- In section two, we elaborate the two population neural field model with external input and discussed in detail the general properties of the model e.g the boundedness property, and the necessary condition for the present choice of the external inputs
- The next one is main section, here we focus on the emergence of persistent activity states under the influence of external input with smooth temporal part. The role of different important parameters such as relative inhibition time, spatial and temporal functions of the external inputs is investigated in detail. It is found that the total duration of the external input and the relative inhibition time constant pays an important role on emergence of the activity in the network.
- In the final part of this study results are discussed and conclusions are drawn accordingly. Numerical simulations in this study are derived on the scheme based on Runge-Kutta fourth order method using MATLAB.

II. MODEL

In the two-population neural field model of co-localized excitatory and inhibitory neurons, we suppose that all these neurons receive synaptic input in the network. This synaptic input depends on the synaptic weights which are dependent of the type and absolute distance between pre-synaptic & post synaptic neurons. The net activity levels in each neurons depends on the weighted sum over the post firing activity in presynaptic neurons. The firing rate of each population at certain time is applicable particular non-linear functions (firing rate function) to the activity levels at the same time. The non-local model in excitatory activity v_e and inhibitory activity level v_i is given as [16], [18], [19]

$$\begin{aligned} v_e &= \alpha_e * \omega_{ee} \otimes F_e(v_e - \phi_e) \\ &\quad - \alpha_i * \omega_{ie} \otimes F_i(v_i - \phi_i) + G_e \qquad (1a) \\ v_i &= \alpha_e * \omega_{ei} \otimes F_e(v_e - \phi_e) \\ &\quad - \alpha_i * \omega_{ii} \otimes F_i(v_i - \phi_i) + G_i \qquad (1b) \end{aligned}$$

where the functions G_m, for $m = e, i$ model the spatio-temporal external inputs. The temporal kernel α_m for $m = e, i$ expresses the impact of past neural firing on the present activity levels in the network. The parameters ϕ_e and ϕ_i are threshold values for firing and the parameter τ stands

for the *relative inhibition time* (ratio between inhibitory and excitatory time constants).

The functions F_m, $(m = e, i)$ stands for firing rate functions. These functions constitute one parameter family of smooth and non-decreasing functions mapped R (the set of real numbers) on to the unit interval [0, 1]. The functions F_m, $(m = e, i)$ are parameterized by a positive steepness parameter β_m. As an example of firing rate function F_m, $(m = e, i)$, we have

$$F_m(v) = \frac{1}{2}(1 + \tanh(\beta_m v)) \tag{2}$$

For $\beta_m \to \infty$ $(m = e, i)$, the firing rate function F_m approaches the Heaviside function Θ:

$$\Theta(v) = \begin{cases} 0, & v < 0 \\ 1, & v \geq 0 \end{cases} \tag{3}$$

The functions ω_{mn}, $(m, n = e, i)$ in (1) are called the connectivity function. These functions model the synaptic connection strength in the network and are assumed to be normalized $(\int_{-\infty}^{\infty} \omega_{mn}(x)dx = 1)$, bounded, symmetric, positive and real valued. The functions ω_{mn} are parameterized by means of *synaptic footprints* $\sigma_{mn}(m, n = e, i)$, i.e

$$\omega_{mn}(x) = \frac{1}{\sigma_{mn}}\Psi_{mn}(\xi_{mn}), \quad \xi_{mn} = \frac{x}{\sigma_{mn}} \tag{4}$$

Here Ψ_{mn} is non-dimensional scaling function. For example, the Gaussian connectivity function of the type (4) is given as

$$\Psi_{mn}(\xi_{mn}) = \frac{1}{\sqrt{\pi}} exp(-\xi_{mn}^2) \tag{5}$$

The operator $\otimes$ in (1) defines the spatial convolution integral, given as

$$[\omega_{mn} \otimes F_m(v_m - \phi_m)](x, t) = \int_{-\infty}^{\infty} \omega_{mn}(x - x')F_m((v_m(x', t) - \phi_m))dx' \tag{6}$$

and the temporal convolution integral $\alpha_{mn} * f$ is given as

$$[\alpha_m * f](x, t) = \int_{-\infty}^{t} \alpha_m(t - t')f(x, t')dt' \tag{7}$$

where the function α_m for $m = e, i$ represent temporal kernels. The common choice for the functions α_m are [3], [14], [16], [18]:

$$\alpha_e(t) = \exp(-t), \quad \alpha_i(t) = \frac{1}{\tau}\exp(-t/\tau) \tag{8}$$

The system of Volterra equations (1) with exponentially decaying temporal kernels is transformed into the following Integro-differential equations [14], [16], [25]

$$\frac{\partial v_e}{\partial t} = -v_e + \int_{-\infty}^{\infty} \omega_{ee}(x - x')F_e(v_e - \phi_e)dx - \int_{-\infty}^{\infty} \omega_{ie}(x - x')F_i(v_i - \phi_i)dx' + G_e(x, t) \tag{9a}$$

$$\tau\frac{\partial v_i}{\partial t} = -v_i + \int_{-\infty}^{\infty} \omega_{ei}(x - x')F_e(v_e - \phi_e)dx' - \int_{-\infty}^{\infty} \omega_{ii}(x - x')F_i(v_i - \phi_i)dx' + G_i(x, t) \tag{9b}$$

by mean of linear chain trick [15]. Finally, the functions G_m, $m = e, i$ model the spatio-temporal external inputs. The general form for the external input is:

$$G_m(x, t) = C_m R_m(x)g_m(t), \quad m = e, i. \tag{10}$$

We have split the external input into three parts, this way we can investigate each part of the external input separately; Here the temporal function $g_m(t)$ shows the time evolution, spatial part $R_m(x)$ with amplitude C_m. Schematically, the model (9) is illustrated in Figure 1.

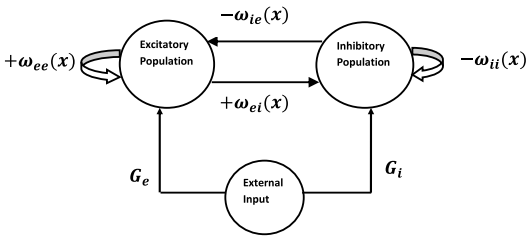

FIGURE 1. Sketch of Two population model (1) with spatio-temporal external input (G_e and G_i).

A. GENERAL PROPERTIES OF THE MODEL

For properly designed connectivity functions, firing rate function and external input functions, for population models one can prove that the initial value problem of (9) is locally wellposed in the space of bounded and continuous functions in a way analogous to Potthast and Graben [35] and Faye and Faugeras [17] for multi-population models with dendritic delay effects and axonal incorporated. The boundedness of solutions to Wilson-Cowan type models have been studied in several papers [3], [14], [35]. Here we prove that the solution of (9) are uniformly bounded subject to both the initial conditions and the external input functions are bounded and continuous.

BOUNDEDNESS

The normalization condition imposed on the connectivity functions ω_{mn} for $m = e, i$ and the function imposed on firing rate functions $0 \leq F_m \leq 1$ reveals the uniform bounds for the convolution integral. By proceeding in a similar way as in Blomquist *et al.* [14] and Potthast and Graben [35] the explicit bounds for the solution v_e and v_i are computed in this subsection. The lower and upper bound functions for excitatory and inhibitory terms for the present choice of temporal function will be same as found in the Yousaf *et al.* [4], which are given as under

$$\text{“}L_l = \alpha_e(t)(U_e(x) + 1) - 1 + [\alpha_e * G_e](x, t) \tag{11a}$$

$$L_u = \alpha_e(t)(U_e(x) - 1) + 1 + [\alpha_e * G_e](x, t) \tag{11b}$$

$$M_l = \tau\alpha_i(t)(U_i(x) + 1) - 1 + [\alpha_i * G_i](x, t) \tag{11c}$$

$$M_u = \tau\alpha_i(t)(U_i(x) - 1) + 1 + [\alpha_i * G_i](x, t)\text{”} \tag{11d}$$

where U_e and U_i are the initial conditions of the system (9), for more detail read the article Yousaf *et al.* [4]. The temporal

convolutions is given as

$$[\alpha_m * G_m](x,t) = \int_0^t \alpha_m(t-s)G_m(x,s)ds \quad m = e,i \tag{12}$$

The functions α_m and G_m are given by (8) and (10), respectively. This convolution for the general temporal function

$$G_m(x,t) = C_m\, R_m(x)\, g_m(t-t_{m0}), \quad m = e,i \tag{13}$$

is transformed into

$$[\alpha_m * G_m](x,t) = C_m R_m(x)\zeta_m(t-t_{m0}) \quad m = e,i \tag{14}$$

where the function ζ_m is given as

$$\zeta_m(t) = \int_{t_{m0}}^t \exp(s/\tau_m)g_m(s)ds \quad m = e,i \tag{15}$$

In this case, we put the value of $g_m(t)$ using as α-type temporal function defined in (26), solve it for the value of ζ. where τ_m is given as

$$\tau_m = \begin{cases} 1, & m = e \\ \tau, & m = i \end{cases} \tag{16}$$

$$\zeta_m(t) = \int_{t_0}^t \exp(s/\tau_m)(d_1 s\exp(-\alpha s))ds \tag{17}$$

$$\zeta_m(t) = d_1 \int_{t_0}^t s\exp(1/\tau_m - \alpha)sds \tag{18}$$

Here d_1 is the normalization constant with respect to area and is given as

$$d_1 = \frac{\alpha^2\exp(\alpha T)}{\exp(\alpha T) - \alpha T - 1} \tag{19}$$

To solve the equation (18), using integration by parts, we end up with the following:

$$\zeta_m(t) = \frac{d_1\tau_m}{(1-\alpha\tau_m)^2}[(t(1-\alpha\tau_m)-\tau_m)\exp(t(1-\alpha\tau_m)/\tau_m) - (t_0(1-\alpha\tau_m)-\tau_m)\exp(t_0(1-\alpha\tau_m)/\tau_m)] \tag{20}$$

After this calculation we end up with

$$\zeta_m(t) = \begin{cases} 0, & t < t_0 \\ \zeta_m^1(t), & t \geq t_0 \end{cases} \tag{21}$$

where

$$\zeta_m^1(t) = \frac{d_1\tau_m}{\lambda^2}[t(\lambda-\tau_m)\exp(t\lambda/\tau_m) - t_0(\lambda-\tau_m)\exp(t_0\lambda/\tau_m)] \tag{22}$$

where $\lambda = 1-\alpha\tau_m$. It is to be noted that these boundedness results are not confined to the Heaviside function only, they holds true for any firing rate function satisfying $0 \leq F_m \leq 1$. The corresponding bounding functions are ploted in Fig. 2. These estimates hold true for continuous external input functions $G_m(x,t)$ with respect to time. The only thing which differs in $g_e(t)$, which also satisfies the same conditions as does in Yousaf *et al.* [4]. Further notice that the arguments produced here hold true even for the case of mutli spatial dimensional neural field models.

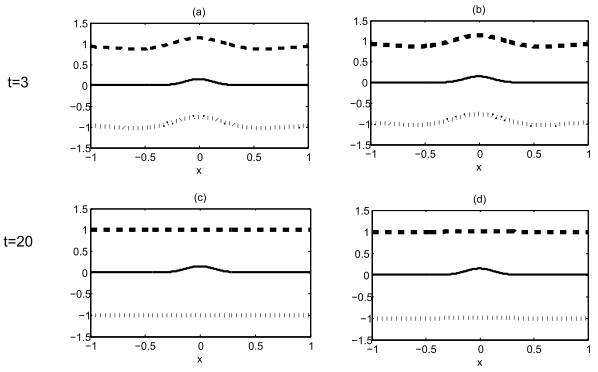

FIGURE 2. boundedness of solutions of the model (9). The black solid, dotted and dash lines represent activity levels, upper and lower bounds, respectively. The left column (a & c) represents excitatory, while the right column (b & d) stands for inhibitory activity and their bounds. Corresponding parameters are shown in table 1 and rest of the parameters are same as used in Fig.3.

TABLE 1. Parameter set for the boundedness property of the solution in Fig.2.

τ	C	T	ϕ_e	ϕ_i
2.5	4	9	.12	.08

B. GENERAL CONDITION ON EMERGENCE OF ACTIVITY

The activity in the network is evoked by the excitatory contribution only. Therefore, we explore the excitatory external input effect only to evoke the activity in the network. In the following Theorem proved in Yousaf *et al.* [3]. "The necessary condition for the external input $G_e(x,t)$ to evoke the activity in the network for model (9) is $G_e(x,t) > \phi_e$" also holds true for the present choice of external input. Next we elaborate in detail about the external input.

C. SPATIO-TEMPORAL EXTERNAL INPUT

The external input is splited into three parts, so that the effect of each part of external input on bumps can be investigated separately, the external input is given as:

$$G_m(x,t) = C_m\, R_m(x)\, g_m(t-t_{m0}), \quad m = e,i \tag{23}$$

where $g_m(t)$ for $m = e,i$ represent temporal function, $R_m(x)$ represent the spatial and C_m is the amplitude of the external input. The spatial functions $R_m(x)$ for $m = e,i$ are continuous and symmetric i.e. $R_m(-x) = R_m(x)$. Symmetry is not necessary for spatial functions, we have not yet tried for it but that can be discussed in future work. The bumps solutions in Fig.3 are two attractor states in present scenario. We have used the set of parameters as used by Bloomquist *et al.* [14], which means that we are in the parameter regime where we have two bump pair solutions. The only objective of this study is to recall or emerge these solutions even though the external input is switched off.

D. SPATIAL FUNCTIONS OF EXTERNAL INPUT

In this work, we have investigated the effect of external input on emergence of the activity using three different spatial functions:

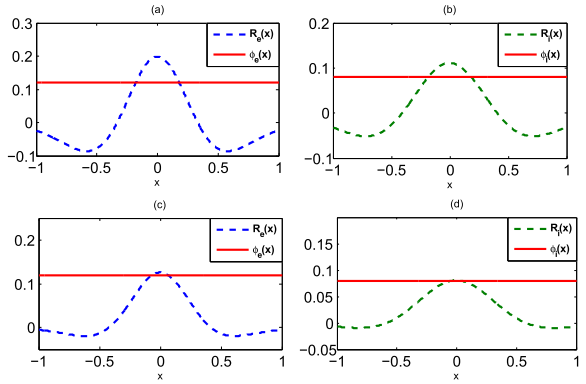

FIGURE 3. Two bump pair solutions with no external input. The first row (a) broad excitatory bump (b) broad inhibitory bump and in the second row (c) narrow excitatory bump (d) Narrow inhibitory bump. The corresponding threshold values are $\phi_e = .12$ and $\phi_i = .08$ and the connectivity functions are assumed to be gaussian as defined in (24). The rest of parameters are shown in Table 2.

TABLE 2. Parameter set for the stationary symmetric solution in Figure 3.

σ_{ee}	σ_{ei}	σ_{ie}	σ_{ii}	ρ_e	ρ_i
.35	.48	.60	.69	.18	.1

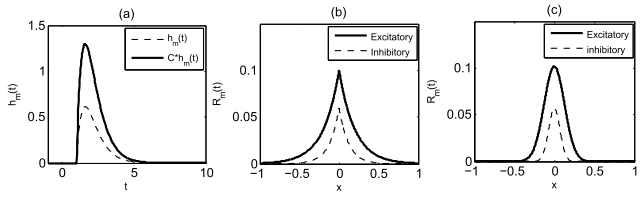

FIGURE 4. The temporal and spatial functions of external input. where dashed and solid curves represent excitatory and inhibitory functions, respectively. (a) α-type temporal function is defined in (26) (b) Gaussian function given by (24). (c) Exponential function given by (25). The corresponding parameters are given in Table 2.

1) One of the stationary symmetric solutions (broad or narrow bump), given in Figure 3.
2) Gaussian function of type (4) given in Figure 4c

$$R_m(x) = \frac{1}{\rho_m\sqrt{\pi}} \exp(-(\frac{x}{\rho_m})^2), \quad m = e, i \tag{24}$$

where ρ_m $(m = e, i)$ is the width parameter.
3) Exponential decay function given in Figure 4b

$$R_m(x) = \frac{1}{2} \exp(-|\frac{x}{\rho_m}|), \quad m = e, i \tag{25}$$

E. TEMPORAL FUNCTIONS OF EXTERNAL INPUT

The temporal functions $g_m(t)$ for $m = e, i$ shown in Figure 4 used in this study to investigate the emergence of the activity are given as:

1) α-type function $g(t)$ is shown in Figure 4a

$$g(t) = \begin{cases} 0 & t < t_0 \\ d_1\ t\ \exp(-\alpha t) & t \geq t_0 \end{cases} \tag{26}$$

where d_1 is the normalization constant with respect to area and is given as

$$d_1 = \frac{\alpha^2 \exp(\alpha T)}{\exp(\alpha T) - \alpha T - 1} \tag{27}$$

The function defined in (26) is α-type function. In order to have a control on the total duration of external input, we assume that

$$g(T) = \varepsilon, \quad \Rightarrow \quad \alpha = -\frac{1}{T}\log(\frac{\varepsilon}{T}) \tag{28}$$

where $\varepsilon = 0.001$ and $T > 0$. This extra condition (28) makes it easier to compare the results with the other type of temporal functions. This type of function is not exactly an α-function but we modified it little bit to control its end point. We have used some conditions e.g. this function is normalized and also satisfy the condition (28). This function will be used as a temporal behavior of the external input. In the study of Roth *et al.* [2], α-type function fits best to sinusoidal input as observed in the experimental data which is more smooth and realistic behavior as compared to triangular one used [4].

III. RESULTS

This is the main section of this study where we investigate the effects of different types of spatio-temporal external inputs (23) the emergence of self-sustained activity states. It is very important to mention here that for case two-population model with no external input [14], there exists two stationary symmetric solutions (bumps) for the present choice of the parameters, one is named as narrow and other is broad. The narrow bump is generally unstable, although the broad bump is stable for suitable values (small and moderate values) of the τ (relative inhibition time) [3], [14]. The stability of these bumps are dependent on relative inhibition time constant τ, The narrow one is unstable for all values of τ, whereas the broad bump is stable if $\tau < \tau_{cr} = 3.01$ [14]. Since the narrow bump solution is unstable and the appearance of the stable activity is actually the broad bump solution of the Wilson-Cowan model with spatio-temporal external inputs.

We investigated the emergence of activity in the network.

A. EMERGENCE OF THE ACTIVITY

Initially, if there is no activity in the network with $G_m(x, t) = 0$, the addition of suitable non-zero excitatory external input $(G_e(x, t))$ can evoke the stable activity, even if the external input is transient, the activity still remains stable. This phenomenon is expressed in Figure 5, which shows the emergence of activity using α-type temporal function and the spatial function $R_m(x)$ of the external input is assumed to be the broad bump. The corresponding excitatory external inputs are given in Figure 5c. The emergence of the activity in the network depends on the spatio-temporal external input. In the next subsection we will explore in detail the effect of each part of the external input separately on bump solutions.

TABLE 3. Parameter set demonstrate the Figure 5, emergence of activity in terms of the amplitude and active time for the external input *G*.

ε	C_e	T_e	ρ_e	ρ_i
0.001	3	6	.18	.1

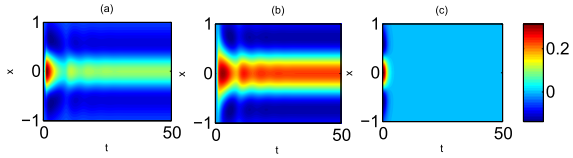

FIGURE 5. Emergence of the activity using α-type function defined in (26) as the temporal part in the external input. The spatial function is assumed to be broad bump. (a) Represents inhibitory activity. (b) stands for excitatory activity in the network. (c) explains corresponding transient excitatory external inputs. The corresponding parameters are: $\varepsilon = 0.001$ and $T_e = 6$, $C_e = 3$. The rest of parameters are same as used in Figure 3.

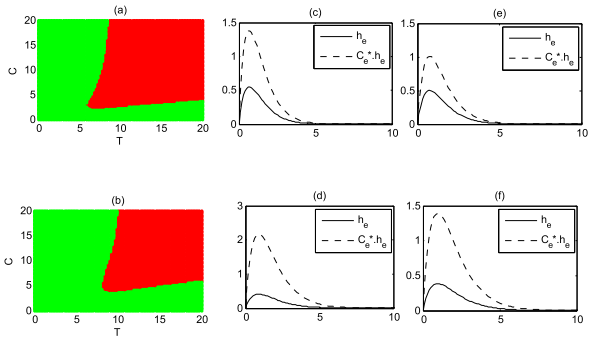

FIGURE 6. Activity appearance as a function of active time *T* and amplitude *C* of the excitatory external input(23) for different spatial functions, while the temporal function is assumed to be the α-type function defined in (26). (a) Broad bump as spatial function (b) Narrow bump as spatial function, (c) and (d) Corresponding temporal functions for smallest amplitude to evoke the activity, while (e) and (f) corresponds to temporal functions for smallest activation time *T* to evoke the activity. Corresponding parameter set is given by Table4. Red color stands for successful activation whereas green color represents no activation.

1) DEPENDENCE ON SPATIAL FUNCTION OF THE EXTERNAL INPUT

The emergence of activity varies for different spatial functions $R_e(x)$ of excitatory external input. In this subsection, we will investigate the emergence of activity for four different types of spatial functions to fixed temporal part (modified α-type function $g(t)$). Fig. 6 and Fig. 7 illustrates the relationship between amplitude and active time of temporal function for the choice of different spatial functions. In the case of broad and narrow spatial functions similar type of behavior is observed. Since broad bump solution is very close to the desired activity (broad bump), which makes it easier to evoke the activity in the network as shown in Fig. 6b, whereas, for narrow bump, larger amplitude and active time T of the external input is required to evoke the activity Fig. 6a. The emergence of activity as a function of amplitude and total duration for exponential and gaussian spatial functions are given in Fig. 7a & Fig. 7b respectively. Both spatial functions shows similar relationship between C and T but for gaussian, it requires smaller value amplitude and T to evoke the activity as it is more similar to the required activity pattern.

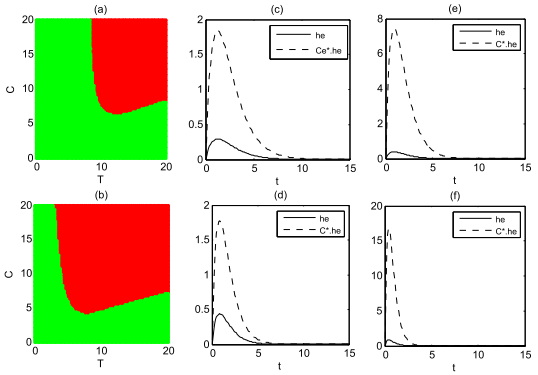

FIGURE 7. Activity emergence as a function of active time *T* and amplitude *C* of the excitatory external input (23) for different spatial functions, while the temporal function is assumed to be the α-type function *g*(*t*). (a) Exponential function as a spatial part of external input and is given by (25) and (b) Gaussian function as a spatial part given by (24), (c) and (d) Corresponding temporal functions for smallest amplitude to evoke the activity, while (e) and (f) correspond to temporal functions for smallest active time of the external input. Red color stands for successful activation whereas green color represents no activation.

TABLE 4. Parameter sets used to demonstrate the emergence of the activity for Fig. 6.

Parameter	Broad BP	Narrow BP
C_e	2.526	4.898
T_e	5.8509	8.163

The corresponding temporal function for lowest amplitude to evoke the activity for each region (amplitude vs Total duration) is shown in Fig.6c & Fig. 6d and in Fig.7c & Fig. 7d, and for lowest active time T is shown in Fig. 7e & Fig. 7f. The spatial functions are even lower than threshold value showing that it is not necessary to have $R(x) \geq \phi$ to evoke the activity in network. Whereas it is necessary the external input $G_e(x,t) \geq \phi_e$ to evoke the activity. This behavior is obvious in the Fig. 7 and mathematically this property has already been proven in Yousaf *et al.* [4].

The minimum value of amplitude and active time required to evoke the activity in network is observed also. In case of the broad bump, the larger range of successful region as compare to narrow bump as a spatial part. The most important fact which we have found in the present work, the minimum value of amplitude C_e is 2.5 and active time is $T_e = 5.8$ required to evoke the activity is less than observed in the previous work [4] this phenomenon is shown in Fig. 6b and parameter set in Table 4. This result strengthens our claim that smooth temporal function is a better choice.

2) DEPENDENCE ON TEMPORAL FUNCTION OF THE EXTERNAL INPUT

Now we investigate the dependence of temporal part $g_e(t)$ of the external input, the spatial part $R_e(x)$ is assumed to be broad bump solution.

The emergence of self sustained activity states are shown in Fig. 8. The red color shows the continual activation of activity states whereas green color shows no activity in the network.

The amplitude vs active time span the axis shown in Fig. 8. We observed the strong dependence of continual activity state

TABLE 5. Parameter sets used to demonstrate the emergence of the activity for Fig.7c & Fig.7d.

Parameter	Gaussian	Exponential
C_e	4.04	6.263
T_e	7.475	11.72

TABLE 6. Parameter sets used to demonstrate the emergence of the activity for Fig. 7e & Fig. 7f, in terms of the amplitude C_e and smallest active time T_e for the external input G.

Parameter	Gaussian	Exponential
T_e	3.465	8.409
C_e	19.27	18.79

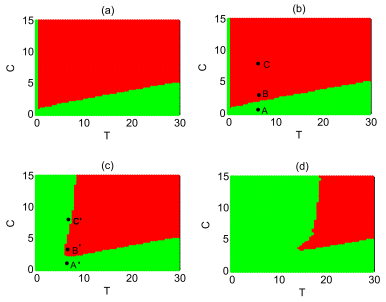

FIGURE 8. Generation of activity as a function of amplitude C_e and stimulus duration time T_e of excitatory external input. Green color represent failure of activation, while red color indicates successful generation. The spatial part $R_e(x)$ of the external input $G_e(x,t)$ is chosen to be broad bump. (a) $\tau = 1.5$, (b) $\tau = 2$, (c) $\tau = 2.5$ and (d) $\tau = 3$. The rest of parameters are same as used in Fig.3. Red color stands for successful activation whereas green color represents no activation.

TABLE 7. Parameter sets used to demonstrate the emergence of the activity for Fig. 8b & Fig. 8c denoted values of points A, B, C, A', B' and C' respectively.

Sr. No.	C	T	τ
point A	1.01	7.071	2
point B	3.636	7.071	2
point C	9.495	7.071	2
point A'	1.01	7.071	2.5
point B'	3.636	7.071	2.5
point C'	9.495	7.071	2.5

for different values of relative inhibitory time constant τ, for the choice of smaller values of τ than τ_{cr} e.g. $\tau = 1.5$ and $\tau = 2.5$, the parameter-plane looks similar shown in Fig. 8a & Fig. 8b. When τ increases 2 to 2.5, there is a wide difference in amplitude vs total duration plane shown in Fig. 8.

Now for one active time T_e, we have three different C_e-regimes in which two of them represents the failure of generation of bump state (marked by A' and C' in Fig. 8c) and one regime between them represents to successful generation (marked by B'). The successful generation region is minimized, when τ is closer to τ_{cr} (see in Fig. 8d), the corresponding pulse width coordinate planes (PWC) planes are shown in Fig. 9. The plot of pulse width coordinates plane in Fig. 9 corresponds to each point A, B, C in Fig. 8b and A', B', C' in Fig. 8c of the temporal evolution of the activity can help to understand this observation. The unsuccessful region indicates by A and A' in Fig. 8b & Fig. 8c respectively

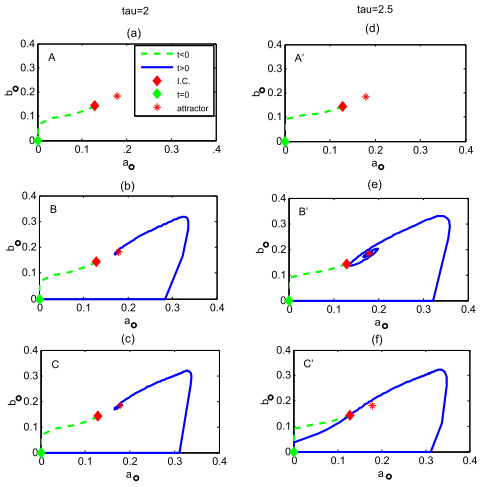

FIGURE 9. Pulse width coordinate evolution in time denoted by points A, B and C in Figure 8b and for points A', B' and C' in Figure 8c. The left column shows PWC for $\tau = 2$ and right column for $\tau = 2.5$.

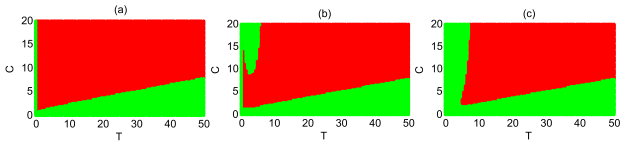

FIGURE 10. The behavior of persistent bump state for three intermediate values of relative inhibitory time constant τ. (a) $\tau = 2.2$, (b) $\tau = 2.3$ and (c) $\tau = 2.4$. The remaining parameters are same as in Figure 3.

and the corresponding PWC are shown in Fig. 9a & Fig. 9d respectively. The red diamond shows the initial condition, which we take the $C_e - T_e$ pair outside the *BOA* (basin of attraction), approaches to trivial point $(a_0, b_0) = (0, 0)$, here we have different choices of pair no evolution (a_0, b_0) from $(0, 0)$ even external input $G_e(x, t)$ in the system but below threshold ϕ_e.

The successful activation indicated by points B and B' in Fig. 8b and Fig. 8c and corresponding PWC behavior is shown in Fig. 9 by blue lines as the excitatory pulse width coordinates becomes greater than or equal to 0.3 (approximately), (blue curve) Fig. 9b & Fig. 9e. At this point inhibitory activity is also evoked, then we observe the inhibitory pulse width coordinate b increasing quickly and move towards the attractor (red $*$). Then establish the persistent activity in the network and the slow inhibition for large value of τ, the behavior seen in Fig. 9e(blue curve).

For the values of points C and C' in Fig. 8b & Fig. 8c observe the prominent difference in two cases for different values of τ Fig. 9c & Fig. 9f. The little bit expedition for the small value of τ in Fig. 9c around the red $*$ and it leave the BOA for large value of τ, coming back to fixed point shown in Fig. 9f.

If we choose the value of $\tau = 2.2$ in Fig. 10a, we have similar view as in Fig. 8b, but for the value of $\tau = 2.3$ failure of activation in small island for larger values of amplitude C_e and smaller values of active time T_e. This region is enlarge, when we increasing the value of τ shown in Fig. 10c for $\tau = 2.4$. The green region shows failure of activity merging

for any amplitude if time duration is small. Our numerical simulations resemble some of the results obtained in Yousaf *et al.* [4] and Folias and Bressloff [30]. In comparison with Folias and Bressloff [30], we investigated the two-population neural model analogous to Wilson Cowan type model [1] subject to spatio temporal external input. Blomquist *et al.* [14] has also studied the same type of model with no external input and found the conditions for existence, uniqueness and stability of stationary symmetric solutions. The generic picture consists of two stationary symmetric solutions (bump pairs), first named as narrow bump pair and the second is named as a broad bump pair. The narrow bump pair is unstable while the broad bump pair is stable for small and moderate values of relative inhibition time constant τ.

IV. CONCLUSIONS AND FUTURE WORKS

The persistent activation of population of neurons in the cortex during the active memory task is one of the best studied neural correlates of higher cognitive function, so called working memory [39, Goldman,1995]. A possible way underlying this type of activation of subpopulations of neurons in the network is the switching between the attractor states, which is found in the neural firing rate models by means of the external input [1], [19], [27], [29].

In this study, Wilson Cowan type two-population neural field model extended with different spatio-temporal external input has been investigated. The model with no external input corresponds to at most two bump pair solutions named as broad and narrow bumps [14]. Narrow bump is generally unstable whereas the broad is stable for suitable values (small and moderate) of relative inhibition time constant τ. The parameters for this study are same as used by Bloomquist *et al.* [14] which means that we are in the parameter regime where we know that there are attractor states (broad and narrow bump pairs) in the network. Initially, if there is no activity in the network, activity (broad bump) can be evoked by switching on suitable transient excitatory external input. This activity remains stable even though external input is switched off this phenomenon is illustrated in Fig.5.

In Yousaf *et al.* [4], the emergence of persistent activity states is explored under the influence of spatio-temoral external input with triangular temporal function. The selection of triangular external input is motivated by the work of Pinto *et al.* [34]. The present work is the continuation of previous work [3] for more smooth temporal function which is more natural behavior of inputs as observed by Roth *et al.* [2] in the visual cortex. The α function fits best for this smooth behavior. In order to have a control on the total duration of the external input, we slightly modified it, that is why we name it as the α-type function given 26. It is more evident and natural behavior that sinusoidal inputs are more likely smooth as compare to triangular. Here, we have investigated the emergence of persistent activity states in response to spatio-temporal external input for different spatial and smooth (α-type) temporal function. The results are summarized as under:

In the first part, we have investigated the boundedness property of the solutions under the influence of external input. Mathematical form for bounds are calculated 21 and is shown numerically in Figure 2. This result shows that the solutions are bounded for finite external input which means that any instability detected has to be saturated. The necessary condition for emergence of the activity discussed in [4] also holds true for the present choice of external input. In the second part, the emergence of persistent activity states is investigated for different choices of spatial functions while keeping α-type as a temporal function in the external input. Four types of spatial functions investigated such as Gaussian, Exponential, narrow and broad bump functions. One can also investigate the emergence of the activity for some other spatial functions. The choice of these functions is made on the basis of their similar behavior to stationary symmetric solutions (persistent activity states) of the model. Fig. 6 shows the emergence of activity as a function of amplitude and total duration of the external input for broad and narrow bumps as spatial functions. In case of broad bump, activity in the network is evoked for smaller values of parameters (**C** and **T**) as compare to case where narrow bump function is used as a spatial function. Similar behavior is observed for the case of Gaussian and exponential spatial functions, this result is illustrated in Fig. 7 which shows that the emergence of the activity is easier for Gaussian function in comparison with exponential one. In all four cases of spatial functions, the broad bump function is a better choice for spatial function in the external input to evoke the activity in the network. Since broad bump is the attractor state in the network, therefore this may be one of reasons that broad bump as a spatial function evokes activity more quickly as compare to others spatial functions.

In the next part, emergence of the activity is investigated as a function of temporal part (α-type function) by keeping broad bump as a fixed spatial part of the external input.

In the systematic variation in external input (spatial function $R_e(x)$ and temporal function $g_e(t)$), the amplitude C_e and total duration time T_e exceed certain threshold values to evoke the persistent activity. It is observed that relative inhibition time constant τ plays an important role in shaping total duration time versus amplitude. It is easier to evoke the activity in network for smaller values of τ as shown in Fig. 8a and Fig. 8b.

The strong dependence of τ on emergence of persistent activity states is observed for our case, the parameter-planes (Amplitude versus total duration) show similar behavior for much smaller values of τ than the critical time τ_{cr}. When the values of τ approaches to τ_{cr}, a remarkable change in amplitude versus total duration plane is observed.

In comparison with triangular type spatio-temporal external input discussed in Yousaf *et al.* [4]. It is found that minimum values of the amplitude and total duration required to evoke the selective persistent states in network is much smaller as found in [4]. This result is shown in Fig. 6b and corresponding parameter set in Table 4. Similarly, the minimum value of total duration T_e required to evoke the

activity in network is (Table 4) also smaller as observed in Yousaf *et al.* [4]. All these results empowers our claim that the temporal behavior ($\alpha - type$) of the external input is more natural behavior observed and more efficient to evoke the activity in the network.

In future work, we intend to investigate the annihilation of persistent activity states for the α-type temporal function. The different aspects of the external input to the model will be investigated to annihilate the activity in network.

ACKNOWLEDGMENTS

The authors would like to thanks Dr. John Wyller, Dr. Gaute T. Einevol, Dr. Birgit Kriener(NMBU) and Dr. Tom Tetzlof (Institute for Advanced Simulation Theoretical Neuroscience) for very useful discussions in preparation of this paper.

REFERENCES

[1] H. R. Wilson and J. D. Cowan, "A mathematical theory of the functional dynamics of cortical and thalamic nervous tissue," *Kybernetik*, vol. 13, no. 2, pp. 55–80, Sep. 1973.

[2] M. M. Roth, J. C. Dahmen, D. R. Muir, F. Imhof, F. J. Martini, and S. B. Hofer, "Thalamic nuclei convey diverse contextual information to layer 1 of visual cortex," *Nature Neurosci.*, vol. 19, no. 2, pp. 299–307, 2016.

[3] M. Yousaf, J. Wyller, G. T. Einevoll, and T. Tetzlaff, "Effect of localized input on bump solutions in a two-population neural-field model," *Nonlinear Anal. Real World Appl.*, vol. 14, no. 2, pp. 997–1025, 2013.

[4] M. Yousaf, B. Kriener, J. Wyller, and G. T. Einevoll, "Generation and annihilation of localized persistent-activity states in a two-population neural-field model," *Neural Netw.*, vol. 46, pp. 75–90, Oct. 2013.

[5] G. Gillary, R. von der Heydt, and E. Niebur, "Short-term depression and transient memory in sensory cortex," *J Comput. Neurosci.*, vol. 43, no. 3, pp. 273–294, Dec. 2017.

[6] K. Kolodina, A. Oleynik, and J. Wyller, "Single bumps in a 2-population homogenized neuronal network model," *Phys. D, Nonlinear Phenomena*, vol. 370, pp. 40–53, May 2018.

[7] A. Richard, P. Orio, and E. Tanré, "An integrate-and-fire model to generate spike trains with long-range dependence," *J Comput. Neurosci.*, vol. 44, no. 3, pp. 297–312, Jun. 2018.

[8] K. Kolodina, V. Kostrykin, and A. Oleynik, "Stationary periodic solutions in the Amari model," in *Proc. Conf. ICMNS*, Juan-les-Pins, France, 2018. doi: 10.13140/RG.2.2.16866.43200.

[9] E. Burlakov, A. Ponosov, and J. Wyller, "Stationary solutions of continuous and discontinuous neural field equations," *J. Math. Anal. Appl.*, vol. 444, no. 1, pp. 47–68, Dec. 2016.

[10] E. Burlakov, E. Zhukovskiy, A. Ponosov, and J. Wyller, "Existence, uniqueness and continuous dependence on parameters of solutions to neural field equations," *Memoirs Differ. Equ. Math. Phys.*, vol. 65, pp. 35–55, Jan. 2015.

[11] C. P. Fall, T. J. Lewis, and J. Rinzel, "Background-activity-dependent properties of a network model for working memory that incorporates cellular bistability," *Biol. Cybern.*, vol. 93, no. 2, pp. 109–118, 2005.

[12] X.-J. Wang, "Synaptic reverberation underlying mnemonic persistent activity," *Trends Neurosci.*, vol. 24, no. 8, pp. 455–463, Aug. 2001.

[13] A. Compte, "Computational and in vitro studies of persistent activity: Edging towards cellular and synaptic mechanisms of working memory," *Neuroscience*, vol. 139, no. 1, pp. 135–151, Apr. 2006.

[14] P. Blomquist, J. Wyller, and G. T. Einevoll, "Localized activity patterns in two-population neuronal networks," *Phys. D, Nonlinear Phenomena*, vol. 206, nos. 3–4, pp. 180–212, Jul. 2005.

[15] N. McDonald, *Time Lags in Biological Models* (Lecture Notes in Biomathematics). Berlin, Germany: Springer-Verlag, 1978.

[16] A. Oleynik, J. Wyller, T. Tetzlaff, and G. T. Einevoll, "Stability of bumps in a two-population neural-field model with quasi-power temporal kernels," *Nonlinear Anal. Real World Appl.*, vol. 12, no. 6, pp. 3073–3094, Dec. 2011.

[17] G. Faye and O. Faugeras, "Some theoretical and numerical results for delayed neural field equations," *Phys. D, Nonlinear Phenomena*, vol. 239, no. 9, pp. 561–578, May 2010.

[18] J. Wyller, P. Blomquist, and G. T. Einevoll, "On the origin and properties of two-population neural field models—A tutorial introduction," *Biophys. Rev. Lett.*, vol. 2, no. 1, pp. 79–98, 2007.

[19] S. Coombes and M. R. Owen, "Bumps, breathers, and waves in a neural network with spike frequency adaptation," *Phys. Rev. Lett.*, vol. 94, pp. 102–148, Apr. 2005. doi: 10.1103/PhysRevLett.94.148102.

[20] E. M. Izhikevich, *Dynamical Systems in Neuroscience: The Geometry of Excitability and Bursting*. Cambridge, MA, USA: MIT Press, 2007. [Online]. Available: https://scholar.google.com.pk/scholar?hl=en&as_sdt=0%2C5&q=E.+M.+Ezhikevitch%2C+Dynamical+Systems+in+Neuroscience%3A+The+Geometry+of+643+Excitability+and+Bursting%2C+Cambridge%2C+MA%2C+USA%3A+MIT+Press.&btnG=

[21] E. K. Miller, C. A. Erickson, and R. Desimone, "Neural mechanisms of visual working memory in prefrontal cortex of the macaque," *J. Neurosci.*, vol. 16, no. 16, pp. 5154–5167, Aug. 1996.

[22] Y. Guo and C. Chow, "Existenc and stability of standing pulses in neural networks: I. Existence," *SIAM J. Appl. Dyn. Syst.*, vol. 4, no. 2, pp. 217–248, 2005.

[23] A. Compte, N. Brunel, P. S. Goldman-Rakic, and X.-J. Wang, "Synaptic mechanisms and network dynamics underlying spatial working memory in a cortical network model," *Cerebral Cortex*, vol. 10, no. 9, pp. 910–923, Sep. 2000.

[24] R. T. Gray and P. A. Robinson, "Stability and structural constraints of random brain networks with excitatory and inhibitory neural populations," *J. Comput. Neurosci.*, vol. 27, no. 1, pp. 81–101, 2009.

[25] J. Wyller, P. Blomquist, and G. T. Einevoll, "Turing instability and pattern formation in a two-population neuronal network model," *Phys. D, Nonlinear Phenomena*, vol. 225, no. 1, pp. 75–93, 2007.

[26] Y. Guo and C. C. Chow, "Existence and stability of standing pulses in neural networks: II," *SIAM J. Appl. Dyn. Syst.*, vol. 4, no. 2, pp. 249–281, 2005.

[27] S. Amari, "Dynamics of pattern formation in lateral-inhibition type neural fields," *Biol. Cybern.*, vol. 27, no. 2, pp. 77–87, 1977.

[28] J. R. Cressman, G. Ullah, J. Ziburkus, S. J. Schiff, and E. Barreto, "The influence of sodium and potassium dynamics on excitability, seizures, and the stability of persistent states: I. Single neuron dynamics," *J. Comput. Neurosci.*, vol. 26, no. 2, pp. 159–170, 2009.

[29] C. R. Laing, W. C. Troy, B. Gutkin, and G. B. Ermentrout, "Multiple bumps in a neuronal model of working memory," *SIAM J. Appl. Math.*, vol. 63, no. 1, pp. 62–97, 2002.

[30] S. E. Folias and P. C. Bressloff, "Breathing pulses in an excitatory neural network," *SIAM J. Appl. Dyn. Syst.*, vol. 3, no. 3, pp. 378–407, 2004.

[31] J. Rubin and A. Bose, "Localized activity patterns in excitatory neuronal networks," *Netw. Comput. Neural Syst.*, vol. 15, no. 2, pp. 133–158, 2004.

[32] J. E. Rubin and W. C. Troy, "Sustained spatial patterns of activity in neuronal populations without recurrent excitation," *SIAM J. Appl. Math.*, vol. 64, no. 5, pp. 1609–1635, 2004.

[33] B. Ermentrout and J. D. Drover, "Nonlinear coupling near a degenerate Hopf (Bautin) bifurcation," *SIAM J. Appl. Math.*, vol. 63, no. 5, pp. 1627–1647, 2003.

[34] D. J. Pinto, J. A. Hartings, J. C. Brumberg, and D. J. Simons, "Cortical damping: Analysis of thalamocortical response transformations in rodent barrel cortex," *Cerebral Cortex*, vol. 13, no. 1, pp. 33–44, Jan. 2003.

[35] R. Potthast and P. B. Graben, "Existence and properties of solutions for neural field equations," *Math. Methods Appl. Sci.*, vol. 33, no. 8, pp. 935–949, May 2010.

[36] J. A. Pava and F. M. A. Natali, "Stability and instability of periodic travelling wave solutions for the critical Korteweg–de Vries and nonlinear Schrödinger equations," *Phys. D, Nonlinear Phenomena*, vol. 238, no. 6, pp. 603–621, 2009.

[37] K. Kishimoto and S. Amari, "Existence and stability of local excitations in homogeneous neural fields," *J. Math. Biol.*, vol. 7, no. 4, pp. 303–318, 1979.

[38] Z. P. Kilpatrick and P. C. Bressloff, "Stability of bumps in piecewise smooth neural fields with nonlinear adaptation," *Phys. D, Nonlinear Phenomena*, vol. 239, no. 12, pp. 1048–1060, 2010.

[39] P. S. Goldman-Rakic, "Cellular basis of working memory," *Neuron*, vol. 14, no. 3, pp. 477–485, Mar. 1995.

[40] Z. P. Kilpatrick and P. C. Bressloff, "Effects of synaptic depression and adaptation on spatiotemporal dynamics of an excitatory neuronal network," *Phys. D, Nonlinear Phenomena*, vol. 239, no. 9, pp. 547–560, May 2010.

ZEESHAN AFZAL is currently a Ph.D. Scholar with the Department of Mathematics, COMSATS University Islamabad, Lahore Campus, Lahore. His research interests include computational neuroscience, differential equations, and graph theory.

YONGSHENG RAO received the B.S. and M.S. degrees in mathematics from Guangzhou University, in 2002 and 2009, respectively, and the Ph.D. degree in engineering from Sun Yat-sen University, in 2017. He is currently a Lecturer with Guangzhou University.

His research interests include graph theory and computer science.

YOUSAF BHATTI received the M.S. and Ph.D. degrees in mathematics from the Norwegian University of Life Sciences (NMBU), Norway, in 2009 and 2013, respectively. His study was funded by the Higher education Commission of Pakistan. He is currently an Assistant Professor with the Mathematics Department, COMSATS University Islamabad, Lahore Campus. He has published his work in top level journals. His current interests include computational neuroscience, medical physics, and graph theory with applications and differential equations. He also received the NRPU Project Award, in 2016.

NAIMA AMIN received the Ph.D. degree in medical physics, in 2011. She did her experiment work at the University of Dundee, Nineswell Hospital, and also at the Medical School, U.K. She is currently an Assistant Professor with the Department of Physics, COMSATS University Islamabad, Lahore Campus. Her research interests include medical physics and computational neuroscience. She has received a couple of projects under NRPU project.